Carbohydrate Research 448 (2017) 136–147

Contents lists available at ScienceDirect

Carbohydrate Research

journal homepage: www.elsevier.com/locate/carres

Exhaustive rotamer search of the $^4C_1$ conformation of α- and β-D-galactopyranose

Enrique A. Del Vigo, Carla Marino, Carlos A. Stortz*

Universidad de Buenos Aires, Facultad de Ciencias Exactas y Naturales, Consejo Nacional de Investigaciones Científicas y Técnicas, Centro de Investigaciones en Hidratos de Carbono (CIHIDECAR), Departamento de Química Orgánica, Pab. 2, Ciudad Universitaria, 1428 Buenos Aires, Argentina

ARTICLE INFO

Article history:
Received 8 March 2017
Received in revised form
3 April 2017
Accepted 5 May 2017
Available online 6 May 2017

Keywords:
Galactose
Conformation
Density functional theory
Rotamer
Exhaustive search
Solvent model

ABSTRACT

An exhaustive search approach was used to establish all possible rotamers of α- and β-D-galactopyranose using DFT at the B3LYP/6-311+G** and M06-2X/6-311+G** levels, both in vacuum calculations, and including two variants of continuum solvent models as PCM and SMD to simulate water solutions. Free energies were also calculated. MM3 was used as the starting point for calculations, using a dielectric constant of 1.5 for vacuum modeling, and 80 for water solution modeling. For the vacuum calculations, out of the theoretically possible 729 rotamers, only about a hundred rendered stable minima, highly stabilized by hydrogen bonding and scattered in a ca. 14 kcal/mol span. The rotamer with a clockwise arrangement of hydrogen bonds was the most stable for the α-anomer, whereas that with a counter-clockwise arrangement was the most stable for the β-anomer. Free energy calculations, and especially solvent modeling, tend to flatten the potential energy surface. With PCM, the total range of energies was reduced to 9–10 kcal/mol (α-anomer) or 7–8 kcal/mol (β-anomer). These figures fall to 4.5–6 kcal/mol using SMD. At the same time, the total number of possible rotamers increases dramatically to about 300 with PCM, and to 400 with SMD. Both models show a divergent behavior: PCM tends to underestimate the effect of solvent, thus rendering as the most stable many common rotamers with vacuum calculations, and giving underestimations of populations of β-anomers and *gt* rotamers in the equilibrium. On the other hand, SMD gives a better estimation of the solvent effect, yielding correct populations of *gt* rotamers, but more β-anomers than expected by the experimental values. The best agreement is observed when the functional M06-2X is combined with SMD. Both DFT models show minimal geometrical differences between the optimized conformers.

1. Introduction

Carbohydrates play a very significant role in biological systems, appearing either as free monosaccharides, oligomeric or polymeric products, alone or combined with other molecules in key functions, as in glycoproteins and glycolipids. The knowledge of the conformational states of carbohydrates is essential to evaluate their biological and physical functions [1], and can be aided by reliable molecular modeling. The presence of mobile hydroxyl and hydroxymethyl groups in the carbohydrate molecules introduce the so-called "multiple mimima problem" [2], which complicates the potential energy surfaces by leading to a lot of local minima, with non-surmountable energy barriers separating them. Even for one anomer of a simple aldohexose in pyranosic form and a fixed chair conformation, the three possible staggered conformations for each of the five hydroxyl groups and the hydroxymethyl group lead to $3^6 = 729$ theoretically possible minima. Although some sterical clashes will occur for some combinations, the starting points for any possible calculation are counted in hundreds. This fact has been overlooked in many studies, thus some true minima may be missing in those calculations. Recently, Mayes et al. [3] studied the conformational pathways from $^4C_1$ to $^1C_4$ of some monosaccharides, passing through envelopes, half-chairs, boats and skew-boats. They have taken a careful consideration to all possible exocyclic rotamers (leading to 38 × 729 starting points for each monosaccharide), and concluded that theoretical studies **must** consider the role of exocyclic groups when constructing kinetic and thermodynamic landscapes. Avoiding this issue may lead to over- or underestimations of energy barriers for puckering [3]. Furthermore, another study showed that the pathways

* Corresponding author.
E-mail address: stortz@qo.fcen.uba.ar (C.A. Stortz).

http://dx.doi.org/10.1016/j.carres.2017.05.003
0008-6215/

involving each of the rotamers should be considered, as many different rotamers present combined pathways for ring inversion [4]. The problem has been recognized since the early flexible residue analysis [5–8], and circumvented in different ways to avoid long computing times: for instance, considering that secondary hydroxyl groups are likely to form a crown of cooperative hydrogen bonds, either clockwise or counterclockwise [9,10], thus using just two starting conformations for these four hydroxyl groups. Heuristic approaches [11,12] and random sampling techniques [8] have also been used. Molecular dynamic simulations also overcome the problem as they can surpass potential barriers. It has been used since the early days of carbohydrate modeling [9,13–15], and is still today the method of choice of many researchers for the conformational analysis of mono- and disaccharides [16,17], sometimes in the form of *ab initio* metadynamics [18]. These shortcuts do not help when a full characterization of the potential energy surface is needed, or when the most important rotamers should be submitted to further calculations. An exhaustive search can be the only way of retrieving such information. However, reports of full conformational searches are scarce. The first works at the quantum level, made with glucose, considered the different rotations for the hydroxymethyl group, but not those of the hydroxyl groups [19]. Cramer and Truhlar [20] studied all the hydroxymethyl rotamers, but also explored the 81 possible secondary hydroxyl rotamers for a given conformation of the hydroxymethyl group at the semiempirical levels AM1 and PM3, including solvation. Later, an AM1 study comprising different rotamers of glucose and galactose was published [21], although it is not clear how these conformers were chosen.

Specifically regarding galactose, a full conformational search for the α-anomer using MM3, AM1 and PM3 was published in 1998 [22]. Later, a study where the four secondary hydroxyl groups start at the X-ray diffraction dihedral angles and the remaining groups were rotated was made at semiempirical and HF/6-31G* levels [23]. The group of Momany studied [24] six conformers of α- and six of β-galactose ($^4C_1$ conformation) produced by rotation of the hydroxymethyl group and by changing the crown of hydrogen bonds from clockwise to counterclockwise, at the B3LYP/6-311++G** level. They also studied the alternate chair and some boat and skew forms [24]. Another study found the most important rotamers of the β-anomer using a Monte Carlo approach, and later optimized them at the B3LYP/6-31+G* level [25]. By a combination of resonant two-photon ionization and resonant ion-dip IR spectroscopy, Jockusch et al. were able to identify the presence of just one major rotamer at low temperatures for phenyl β-D-galactopyranoside [26,27]. The great stability of this conformer and other minor accompanying structures was confirmed by B3LYP/6-31+G* optimization and MP2/6-311++G** energy calculations [26,27]. Csonka has published in the web the structures for galactose calculated with HF [26], but the data appears not be available by now.

In the current work, we have made a full conformational search for the 729 potential rotamers of the $^4C_1$ conformations of α- and β-D-galactopyranose (Fig. 1) with MM3 [28,29] at dielectric constants 1.5 and 80 to emulate vacuum and solution conditions. The resulting set of conformers was optimized by DFT calculations with the functionals B3LYP [30] and M06-2X [31] at the 6-311+G** level as vacuum calculations and with the addition of the polarizable continuum model (PCM) [32] and the SMD model [33] with water as the solvent. Free energies were also calculated. The conformer ensembles obtained in each case were compared to reflect the characteristic features of each method and the true landscape for the galactose rotamers.

2. Methods

2.1. Calculations

Molecular mechanics calculations were carried out using the program MM3(92) (QCPE, Indiana, USA) [28,29] with relevant parameters modified as in the MM3(2000) version [34]. Also, the maximum atomic movement at each step of minimization was reduced from 0.25 to 0.10 Å. The structures were minimized using the block diagonal method, with a termination condition 300 times tighter than the MM3 default. From a given local minimum, an automated routine [22] was used to generate the 729 starting conformations produced by rotation of ±120° for each of the exocyclic dihedral angles. The procedure was carried out twice with different starting points. After removing the repeated conformers, the sets calculated at $\varepsilon = 1.5$ were submitted to DFT optimizations at the B3LYP/6-311+G** and M06-2X/6-311+G** levels. Following the same procedure, the sets obtained after MM3 calculations at $\varepsilon = 80$ were submitted to the same levels of DFT calculation, but optimized separately including PCM [32] and SMD [33] in water. Quantum mechanical calculations were carried out using Gaussian 09W (rev. C.01) [35], with standard termination options.

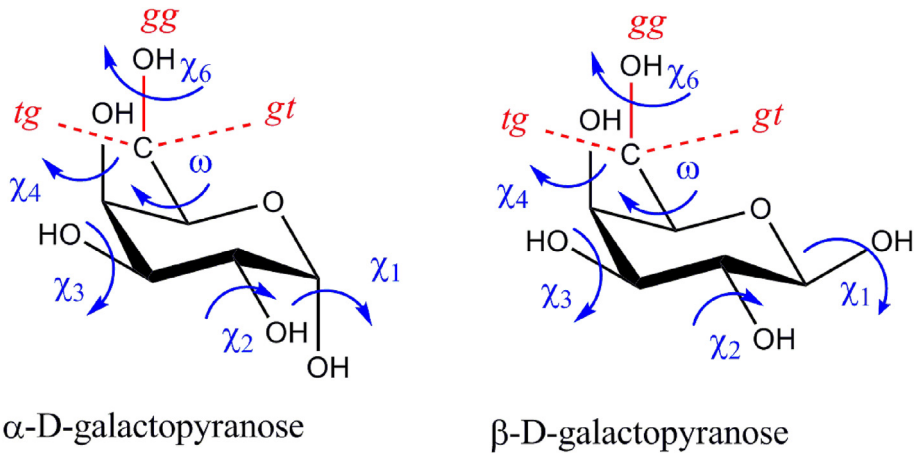

Fig. 1. Schematic representation of α- and β-D-galactopyranose and the torsion angles. For the O-5–C-5–C-6–O-6 torsion angles, the commonly used conformation names *gg*, *gt*, and *tg* are shown.

In either MM3 or DFT calculations, stationary points were characterized by frequency calculations in order to verify that the minima had no imaginary frequencies. When a transition state was detected (it occurred sometimes with MM3 calculations), it was removed from the minima set. For DFT methods, free energies were calculated at 298 K as reported in the Gaussian output file, without scaling. In this way, for each anomer of D-galactopyranose we obtained eight sets of minima: MM3 ($\varepsilon = 1.5$), B3LYP and M06-2X representing gas phase calculations, and MM3 ($\varepsilon = 80$), B3LYP and M06-2X with inclusion of two different solvent models to represent solution calculations. For each set, a list of energies, free energies (for DFT methods) and dihedral angles have been issued, and are provided as a Supplementary Material.

Population analysis was carried out using the Boltzmann equation, with a temperature of 298 K and using free energies for DFT methods and steric energy for MM3. The populations of each rotamer with a given trait were summed to give the whole population with that characteristic.

2.2. Nomenclature

The orientations of the exocyclic secondary hydroxyl groups are indicated by the dihedral angle χ_n, defined by the atoms H-*n*–C-*n*–O-*n*–H(O)-*n*, with $n = 1$ to 4. The angle χ_6 is defined by the atoms C-5–C-6–O-6–H(O)-6 and ω by the atoms O-5–C-5–C-6–O-6. The values for all those angles are described by a one letter code [4,12]: **g** for 5–100°, **T** for angles with absolute value larger than 150°, and **G** for angles between −5° and −100°. No angle values outside these ranges were encountered. The whole conformation for each rotamer is indicated as $\chi_1\chi_2\chi_3\chi_4\ \omega\chi_6$. In the literature, for the ω angle, the acronyms *gg*, *gt* and *tg* are used for what we call **G**, **g** and **T**, respectively (Fig. 1).

For the definition of relative energies and related parameters, we have used the conventions of Csonka et al. [36].

$$\Delta E_{model}\left(conf_i,\ conf_{ref}\right) = E_{model}(conf_i) - E_{model}\left(conf_{ref}\right)$$

i.e. the relative energy is the difference between the energy of the *i*th conformer and the energy of a reference conformer, using the given model chemistry.

$$\Delta\Delta E_{model\ A-model\ B}\left(conf_i,\ conf_{ref}\right) = \Delta E_{model\ A}\left(conf_i,\ conf_{ref}\right) - \Delta E_{model\ B}\left(conf_i,\ conf_{ref}\right)$$

is the difference between the relative energies of the *i*th conformer calculated with two different model chemistries.

The model and reference conformer dependent mean deviation (MD) is defined as:

$$MD_{model\ A-model\ B}\left(conf_{ref}\right) = \frac{1}{n}\sum_{i=1}^{n}\Delta\Delta E_{model\ A-model\ B}\left(conf_i,\ conf_{ref}\right)$$

and the model and reference conformer dependent mean absolute deviation (MAD) is defined as

$$MAD_{model\ A-model\ B}\left(conf_{ref}\right) = \frac{1}{n}\sum_{i=1}^{n}\left|\Delta\Delta E_{model\ A-model\ B}\left(conf_i,\ conf_{ref}\right)\right|$$

Finally, the range of the relative difference, *RRD* is defined as $\max \Delta\Delta E - \min \Delta\Delta E$.

In every case, the reference conformer was that with the lowest free energy determined with the B3LYP functional.

3. Results and discussion

From a given structure of α- and β-D-galactopyranose, rotations around the six exocyclic angles were performed, in order to have 729 starting points for minimizations (full conformational search). They were minimized with the empirical force field MM3, which showed good results for carbohydrates [34]. Calculations were carried out at a dielectric constant value of either 1.5, to simulate vacuum conditions, or 80, to damp electrostatic and hydrogen bonding interactions, and thus to simulate aqueous solutions. Each of the four resulting set of conformers (after eliminating duplicates) was submitted to DFT optimizations at the B3LYP/6-311+G** and M06-2X/6-311+G** levels, with inclusion for the $\varepsilon = 80$ sets of the polarizable continuum model (PCM) and the SMD model using the parameters for water. As expected, many of the 729 starting conformers have clashing substituents. Thus, these conformers led to other, sterically more stable conformations, leading to a considerable decrease in the number of conformers in each set. Furthermore, for the vacuum calculations, hydrogen bonding interactions were strong enough to drive sterically feasible conformations to others stabilized by these H-bonds. In the process of submission of the MM3 sets to DFT calculations, most of the conformers kept approximately the same combination of exocyclic angles as the original MM3 rotamer. However, there were always some conformers which changed one or more of the angles to converge with another rotamer already found, or to generate a new, different rotamer. This process was sometimes the same for both functionals, and sometimes different. The results for each set are presented separately.

3.1. Vacuum calculations for α-D-galactopyranose

Out of the 729 possible rotamers, MM3 optimization ($\varepsilon = 1.5$) led to about 130 conformers. However, control of the imaginary frequencies showed that some were actually transition states. Besides, stringent optimization of some conformers led to convergence with another rotamer. Thus, 117 stable minima were found. Further optimization by DFT led to 113 stable B3LYP minima, and 113 stable M06-2X minima. However, these minima did not correspond to the same conformers. There were 107 conformers common to the three models, 5 appearing for MM3 and M06-2X, 2 appearing for MM3 and B3LYP, 1 appearing for M06-2X and B3LYP, three appearing only for MM3, and three appearing only for B3LYP, making a grand total of 121 different conformers. Giving the procedure employed, starting from MM3, it may sound unusual to find out a DFT minimum which does not have a correspondence in MM3. One of these conformers (**GgGg TG** in the used nomenclature) appeared as a transition state in MM3, in a very flat region of the potential energy surface. However, it optimized sharply by DFT. Three of the minima appearing distinguished in MM3 and B3LYP differ in the value of χ_6: they are **T** for MM3 and **g** for B3LYP. Two of them converged with a third minimum with M06-2X. Anyway, this only happened with some high-energy rotamers. Only one rotamer with low energy did not appear with the three models: it corresponds to the conformer **ggTG GT** (B3LYP $\Delta G = 1.83$ kcal/mol) which, when submitted to optimization by M06-2X converged with the global minimum (**ggTG Gg**) by rotation of χ_6. The 117 MM3 conformers appeared in an energy range of 12.6 kcal/mol. The 113 B3LYP conformers appeared in an energy range of 14.1 kcal/mol, value reduced to 11.9 kcal/mol when free energy was calculated. Those values rise to 15.3 and 13.5 kcal/mol with M06-2X. The DFT methods found as the

Table 1
The five most stable conformers for the $^4C_1$ shape of α- and β-D-galactopyranose, calculated using different methods (vacuum calculations/ε = 1.5).

Conformer	Relative energy (kcal/mol)[a]				
	B3LYP ΔG	B3LYP ΔE	M06-2X ΔG	M06-2X ΔE	MM3 ε = 1.5
α-D-Galp					
ggTG Gg	0.00 (1)	0.00 (1)	0.00 (1)	0.00 (1)	1.64 (5)
GTgg gG	0.27 (2)	0.82 (2)	0.80 (2)	1.51 (2)	0.00 (1)
GTgg Tg	1.10 (3)	1.58 (4)	1.63 (3)	1.72 (3)	
GTgg GG	1.27 (4)	1.45 (3)	1.81 (4)	2.06 (4)	0.13 (2)
GTgg TT	1.35 (5)				
GgTG Gg		1.99 (5)	2.14 (5)	2.26 (5)	1.05 (3)
GTgg gT					1.44 (4)
β-D-Galp					
gGgg gG	0.00 (1)	0.00 (1)	0.00 (1)	0.03 (2)	0.00 (1)
TGgg gG	0.29 (2)	0.23 (2)	0.22 (2)	0.19 (4)	0.96 (3)
gGgg Tg	0.77 (3)	0.62 (4)	0.48 (3)	0.00 (1)	
gGgg GG	1.08 (4)	0.82 (5)			0.20 (2)
gGgg TT	1.12 (5)				
GgTg Gg		0.61 (3)	0.56 (4)	0.03 (3)	
TGgg Tg			0.73 (5)	0.36 (5)	
TGgg GG					1.38 (4)
gGgg gT					1.41 (5)

[a] Rank number for each conformer is given in parenthesis.

global minimum the conformer with a clockwise arrangement of secondary hydrogen bonds which continues from HO-4 to O-6 and from HO-6 to O-5 (conformer **ggTG Gg**, Table 1, Fig. 2a). This was also the lower energy minimum found by Momany et al. (named as α-*gg*-c) [24] with B3LYP/6-311++G**, although no exhaustive search was carried out in that publication. Second in rank, the DFT methods placed the conformer with the corresponding counterclockwise arrangement of hydrogen bonds (**GTgg gG**). It carries an energy 0.82 kcal higher in B3LYP, and 1.51 kcal higher in M06-2X. When free energies were calculated, these values decreased to 0.27 and 0.80 kcal, respectively. This conformer was also predicted to be stable by Momany et al. (α-*gt*-r) [24]. Third and fourth in rank, two other conformers with a counterclockwise arrangement of hydrogen bond appeared; they were differentiated from the second by the orientation of the hydroxymethyl group (Table 1). These four rotamers completed the first 2 kcal of the M06-2X free energy calculations. B3LYP gave rise to four rotamers more within this energy range. On the other hand, MM3 tended to favor counterclockwise arrangements, and to penalize ω = **T** (*tg*) arrangements. Thus, the conformers ranked second and fourth by DFT, appeared as the most stable. In a previous study [22] carried out by MM3 at ε = 3, the two most stable conformers were the same as those found here by DFT methods. The MM3 penalization for ω = **T** (*tg*) arrangements is originated in the torsional potential function for O–C–C–O sequences, which has a minimum at 180° that is 1.3 kcal higher in energy than those at ± 70°. Table 1 shows the five most stable conformers found by each model. The X-ray diffraction structure for this compound (**GTgg TT**) [23,37] matched that ranked fifth with B3LYP (Table 1). However, as several intermolecular hydrogen bonds occur in the monocrystal [37] the exocyclic angles may not be compared fully with calculations on isolated molecules, capable of performing only intramolecular bonds. Besides, the actual orientation of the hydroxyl groups in the crystal is controversial [38]. Fig. 3 depicts the energy values obtained by the different methods for each of the 107 conformers found for all of them. The plot shows that the energy orders are not changed sharply when switching between both DFT functionals or by using free or electronic energy. On the other hand, MM3 shows a different behavior, with many observable "bumps" in the plot, due to larger energy differences. This may be quantified by the mean absolute deviation (MAD) and the range of relative difference (RRD) between each model (Table 2). The MAD values for MM3 against the four DFT calculations are 1.39–2.96 kcal/mol. The worst agreement occurs against the electronic energy by M06-2X. The RRD values are higher than 5 kcal/mol (Table 2). As mentioned above, the strong penalization given by MM3 to ω = **T** (*tg*) rotamers is partly responsible for these differences. The MD values indicate if the energy differences are random, or if some trend occurs. Results indicate that MM3 tends to give lower energy (*i.e.* flatten the surface); however, when comparing with free energies, these values level off. The MAD values between B3LYP and M06-2X are much lower: 0.65–0.91 kcal/mol, and the RRD values are quite much lower: 1.56–1.98 kcal/mol. The MD parameters show that always B3LYP gives lower energy values than M06-2X. In other words, M06-2X shows a better stabilization of the global minimum. When comparing the electronic and free energies for each functional, MAD values of 0.90–1.16 kcal/mol are obtained, together with RRD values of 2.18–2.23 kcal/mol. The MD values show that free energy calculations gave lower relative energies, confirming (Table 1) that the global minimum is entropically less favored. The three conformers previously determined [21,22] as the most stable by the semiempirical method AM1 are ranked 29, 8 and 72 with DFT free relative energies of 4.04–4.39, 2.08–2.42, and 5.78–6.02 kcal/mol, indicating that AM1 fails for the calculation of carbohydrates. The

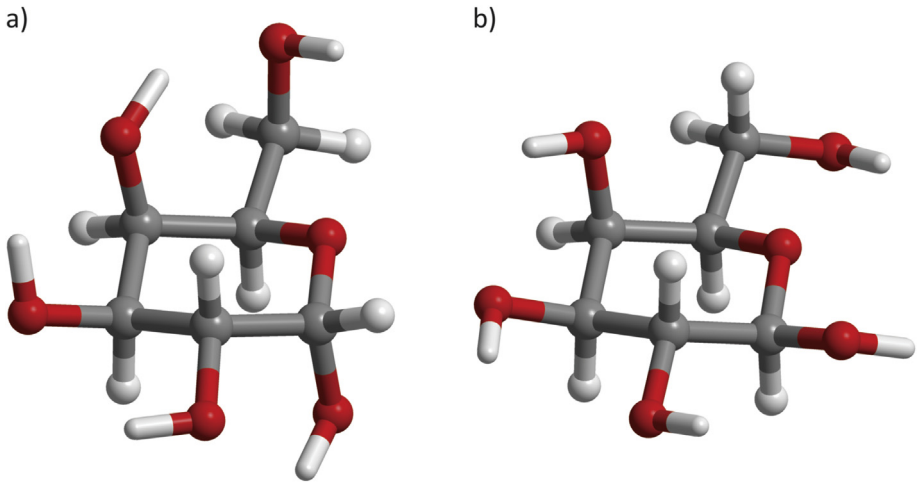

Fig. 2. Structure of the most stable conformers determined by B3LYP/6-311+G** vacuum calculations for a) α-D-galactopyranose, and b) β-D-galactopyranose.

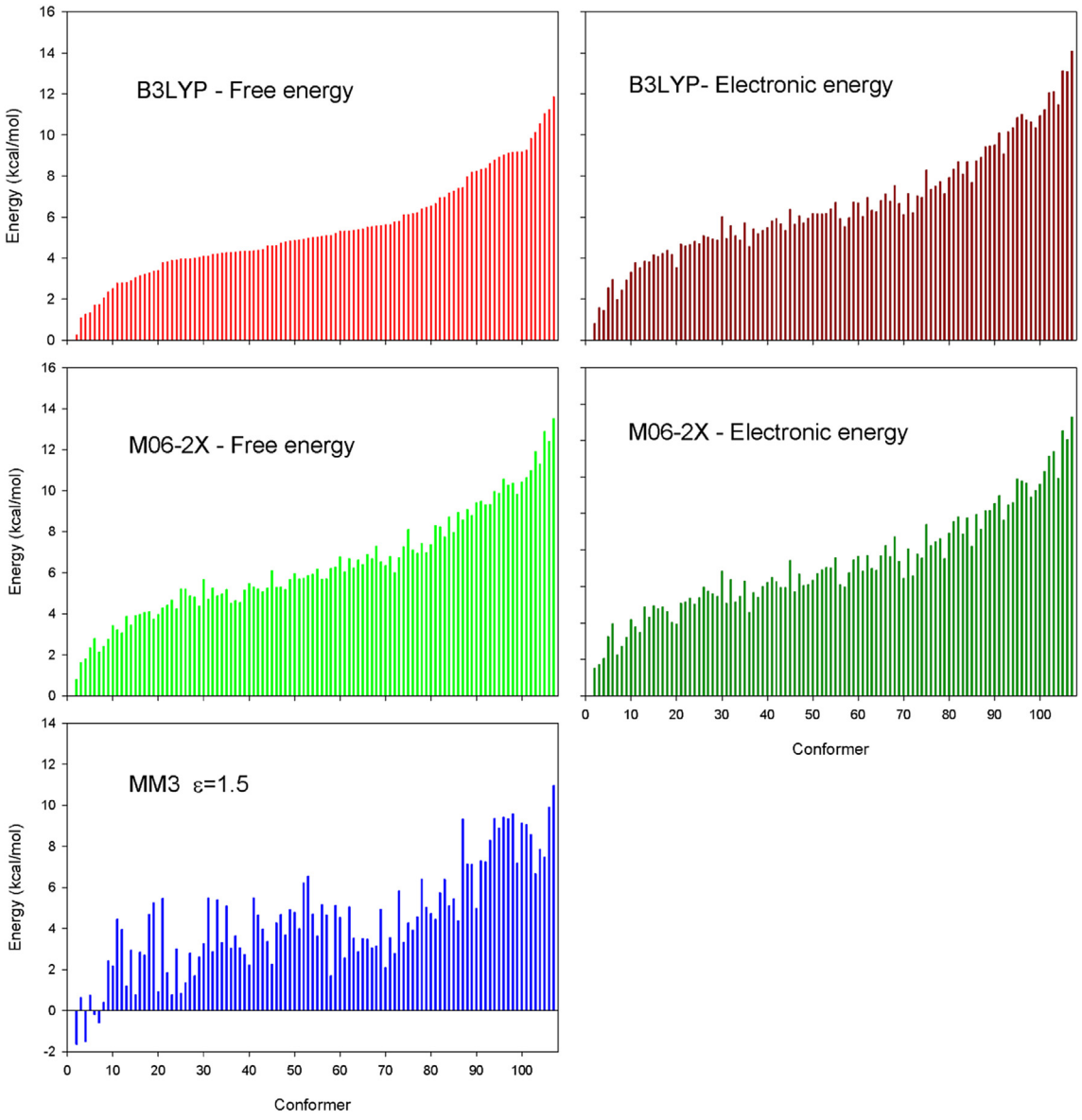

Fig. 3. Representation of the energy of the 107 rotamers of α-D-galactopyranose obtained using each method, sorted according to their relative free energy calculated by B3LYP/6-311+G**.

Table 2
Comparison of the relative energies (in kcal/mol) obtained by different models, as determined by the mean absolute deviations (MAD), mean deviations (MD), and ranges of relative differences (RRD).

Model A	Model B	α-Gal*p*, vacuum		β-Gal*p*, vacuum		α-Gal*p*, SMD water		β-Gal*p*, SMD water		α-Gal*p*, PCM water		β-Gal*p*, PCM water	
		MAD (MD)	RRD	MAD (MD)	RRD	MAD (MD)	RRD	MAD (MD)	RRD	MAD (MD)	RRD	MAD (MD)	RRD
ΔE B3LYP	ΔE M06-2X	0.65 (−0.64)	1.56	0.30 (−0.06)	1.76	0.14 (+0.05)	0.85	0.12 (−0.03)	0.71	0.23 (−0.12)	1.31	0.26 (−0.16)	1.43
ΔG B3LYP	ΔG M06-2X	0.91 (−0.91)	1.98	0.33 (−0.14)	2.37	0.37 (+0.20)	2.77	0.52 (+0.50)	2.42	0.45 (−0.43)	1.75	0.40 (−0.38)	1.71
ΔE B3LYP	ΔG B3LYP	1.16 (+1.16)	2.23	0.55 (+0.42)	3.00	1.08 (−1.07)	3.26	1.01 (−1.01)	2.74	0.51 (+0.37)	2.25	0.39 (+0.20)	2.78
ΔE M06-2X	ΔG M06-2X	0.90 (+0.90)	2.18	0.51 (+0.37)	2.37	0.94 (−0.92)	3.12	0.54 (−0.48)	2.75	0.29 (+0.06)	1.85	0.31 (−0.03)	2.37
MM3	ΔE B3LYP	2.29 (−2.19)	6.72	0.96 (+0.50)	5.48	1.24 (+0.45)	7.75	1.09 (+0.37)	7.03	1.93 (−1.77)	8.44	1.12 (−0.54)	7.21
MM3	ΔE M06-2X	2.96 (−2.90)	8.28	1.17 (+0.39)	7.24	1.23 (+0.48)	7.74	1.08 (+0.33)	6.99	2.13 (−1.96)	9.34	1.32 (−0.75)	8.21
MM3	ΔG B3LYP	1.39 (−1.04)	5.45	1.15 (+0.91)	4.37	1.02 (−0.63)	5.88	1.06 (−0.64)	6.23	1.53 (−1.39)	7.13	0.94 (−0.34)	6.32
MM3	ΔG M06-2X	2.15 (−2.00)	6.91	1.11 (+0.75)	5.52	0.99 (−0.44)	6.51	0.90 (−0.15)	5.66	2.00 (−1.90)	8.92	1.16 (−0.77)	6.81

match with the best conformers [22] obtained by PM3 is not better: they are ranked 29, 9, and 89 in the current B3LYP free energy calculations. It has been stated a long time ago that PM3 fails for sugar modeling [39].

3.2. Vacuum calculations for β-D-galactopyranose

The same procedure already stated for α-galactose generated in this case 116 stable MM3 minima. Further optimization by DFT led to 106 stable B3LYP minima, and 108 stable M06-2X minima. Once more, these minima did not correspond to the same conformers. There were only 100 conformers common to the three models, and a grand total of 120 different conformers. Two of the MM3 conformers carrying $\chi_6 = \mathbf{T}$ rotated this angle to **g** when submitted to the M06-2X minimization, but kept this conformation using B3LYP. The relative energy of most of the conformers was lower than that observed for α-galactose. However, there were a few outliers. All but one of the MM3 conformers appeared in an energy range of 10.6 kcal. Most of the B3LYP conformers appeared in an energy range of less than 9 kcal, value reduced to 8 kcal when free energy was calculated. However, one conformer appeared out of this range by about 4 kcal/mol. Something similar happened with M06-2X, but in this case there were two outliers (one of them not paired with a B3LYP conformer). Fig. 4 shows the energy profiles using

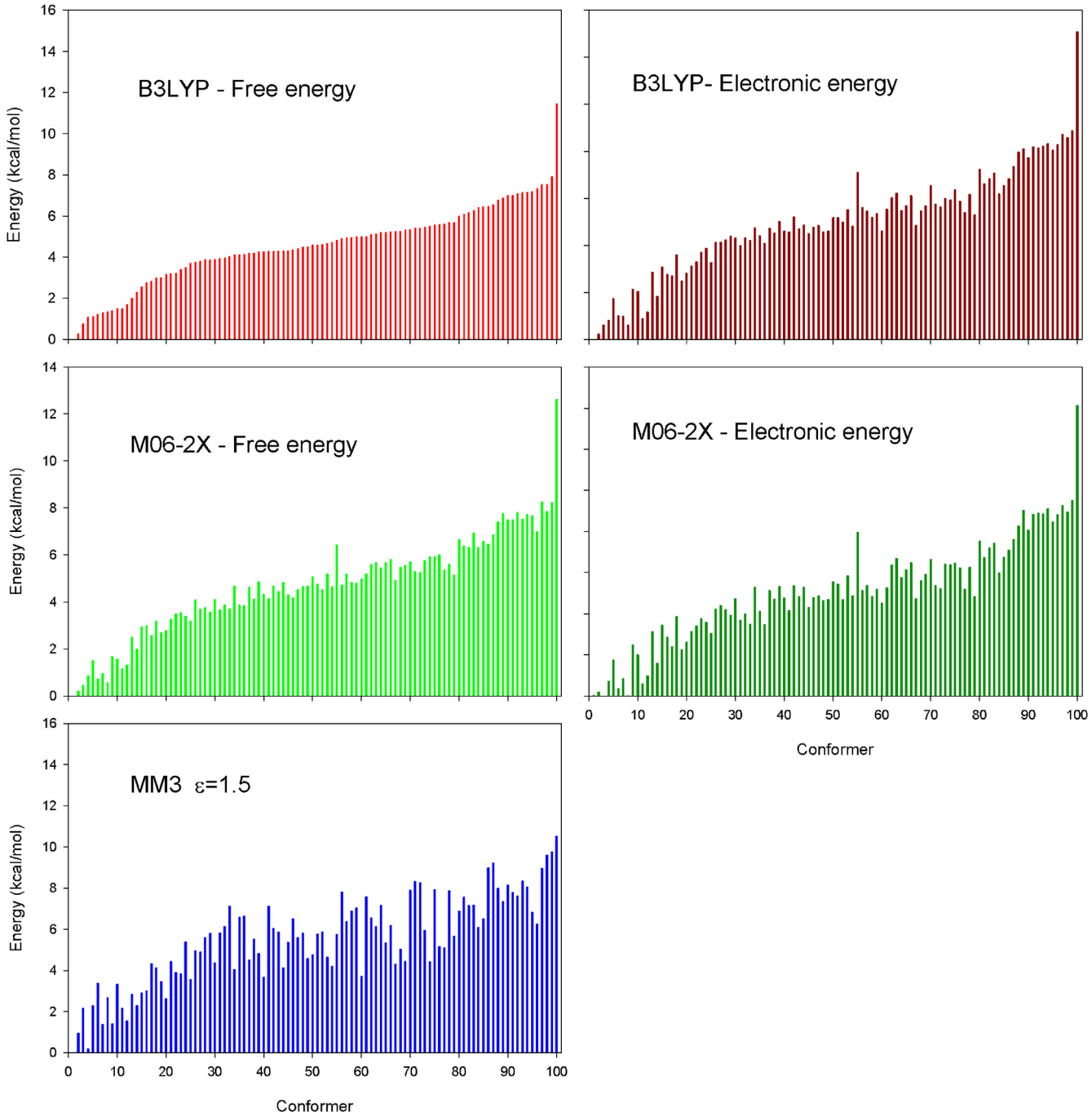

Fig. 4. Representation of the energy of the 100 rotamers of β-D-galactopyranose obtained using each method, sorted according to their relative free energy calculated by B3LYP/6-311+G**.

each method for the 100 common rotamers. This outlier can be clearly observed as the last conformer in the Figures for the DFT models. The Figure also shows that conformer 56 (**ggGg gT**) appears with an energy much higher than those of the surrounding conformers for the M06-2X and B3LYP electronic energy calculations. This is actually due to an unusual stabilization of this conformer by determination of its B3LYP free energy, given by an abnormally high entropy and low zero-point energy. All methods found as the global minimum the conformer with a counterclockwise arrangement of secondary hydrogen bonds which starts from HO-6 to O-4 and finally from HO-1 to O-5 (conformer **gGgg gG**, Table 1, Fig. 2b). This was also the lower energy minimum found by Momany et al. (named as β-*gt*-r) [24] with B3LYP/6-311++G**, and also by Sturdy et al. in a lower level calculation [25]. Furthermore, the group of Simons found [26,27] an equivalent conformer of phenyl β-D-galactopyranoside (where the value of χ_1 is not taken into account due to the presence of the large phenyl substituent) using MP2 calculations; experimentally this conformer appears almost solely at low temperatures [26,27]. The other two conformers observed experimentally in lower amounts (**?Ggg Tg** and **?gTg Gg**, where the **?** indicates that χ_1 is not considered) also match with those appearing in Table 1, although with different energy levels. Results show that several variants of the counterclockwise arrangement for secondary hydroxyl groups were highly preferred by every calculation method. Only one conformer corresponding to a clockwise arrangement (**GgTG Gg**) appeared within the five more stable using M06-2X and by electronic energy determination with B3LYP. The M06-2X calculation actually led to three low-energy conformers with similar energy, namely **gGgg gG**, **gGgg Tg**, and **GgTG Gg**. Free energy calculations established back the differences observed with other models (Table 1). A calculation made by HF/6-31* for β-galactose has failed to found the global minimum, as it started [23] from an orientation of the secondary hydroxyl groups allegedly appearing in the crystalline state [40] but not observed in any of the conformers obtained in the current work. Anyway, the authors [23] reported that in some cases the original orientation **GTgg** for these angles rotated spontaneously by minimization to **TGgg**, which is more likely to occur (Table 1). Taking into account this rotation, the authors assumed that independently from the starting point for the secondary hydroxyl groups, the most stable conformation was obtained [23]. Clearly, this did and does not happen. Some barriers may be overcome during the minimization processes, but many others cannot be overcome. In comparison with the calculations for α-galactose, much more low energy conformers appeared. This may be examined by comparison of Figs. 3 and 4: in the latter the 2 kcal-limit is extended for many more conformers. Fig. 4 shows a better match between the different models than that observed in Fig. 3 for α-galactose. This is observed even better with the deviation parameters (Table 2). The MAD values involving comparison of DFT models are considerably lower than those for α-galactose, indicating small differences not only between B3LYP and M06-2X but also between the usage of free energies or electronic energies (0.30–0.55 kcal/mol, Table 2). The comparison of MM3 with DFT electronic energies also lead to much lower MAD values with regards to α-galactose, as well as lower RRD values. The MD values are also different to those observed for α-galactose: B3LYP no longer gives lower energy values than M06-2X, but the differences are more random, as shown by the low MD value. However, when comparing for each functional the electronic and free energies, it is maintained that free energy calculations give lower relative energies, as the MD values are positive. However, the differences are less patent than for α-galactose. It is worth noting that MM3 shows positive MD values for the four comparisons, indicating that the empirical method actually gives (in average) higher relative energy values than DFT methods. Only two of the three conformers determined previously [21] as the most stable by the semiempirical method AM1 appear in the current search: they are ranked 21 and 22 with B3LYP free relative energies of about 3 kcal/mol.

3.3. Solvent-simulated calculations for α- and β-D-galactopyranose

With $\varepsilon = 80$, out of the 729 possible rotamers, MM3 optimization leads to 433 (α)-435 (β) conformers. The hydrogen bond does not drive any more the optimization, and thus, most of the sterically possible rotamers appear. Further optimization by DFT with inclusion of water by the PCM model, leads to 283-284 stable B3LYP minima, and 286-287 stable M06-2X minima, whereas the use of SMD yielded all the MM3 conformers (433-435) as stable by M06-2X, and just four less by B3LYP. As shown, the values are highly similar between both anomers. The simple landscape observed using SMD is complicated with PCM: about 80 of the DFT minima for the α-anomer have turned the χ_1 dihedral angle from the MM3 minima from a value of ca. 167° to a value of 85° (i.e. from **T** to **g**). These 80 minima did not appear with MM3. Thus, for the α-anomer, only 192 rotamers appear for the three methods, and the grand total of conformers is 524. On the other hand, for the β-anomer, there are 276 common rotamers, and a grand total of 439. Besides increasing the number of available rotamers, the effect of adding a solvent model is a marked decrease in the energy ranges by either method. When adding the solvation model, the DFT energy ranges have decreased from 11.9 to 15.3 kcal/mol to 8.7–10.0 kcal/mol for α-galactose with PCM, and just to 5.4–6.3 kcal/mol with SMD. These figures, for β-galactose are 11.5–14.1 kcal/mol for vacuum calculations, 6.6–8.2 kcal/mol with the PCM model, and 4.2–5.3 kcal/mol with the SMD model. The average energies have decreased in the same proportion. The flattening of the potential energy surface with water modeling is clearly evidenced, and it is significantly larger with the SMD model, which levels off the energies of the different conformers. This flattening has already been observed in other carbohydrate studies [20], but also in other biomolecules, like proteins [41]. Results show that the energy ranges are even smaller for the β-anomer, as already observed for vacuum calculations. It is noteworthy that free energy calculations introduces an additional flattening in vacuum calculations (Section 3.1) and using the PCM model, but the effect is reversed using the SMD model. There is a good correlation between the rotamer energies of both functionals, but the correlation is very poor with the MM3 ($\varepsilon = 80$) calculations. Although some matching conformers appear, the minima found using PCM and SMD are not alike. PCM found global minima akin to the low energy rotamers in vacuum calculations: for the α-anomer, the free energy global minimum is the conformer with a counterclockwise arrangement of secondary hydrogen bonds (**GTgg gG**), which ranks second in vacuum calculations. Other low energy conformers (Table 3) are ranked within the eight most stable rotamers in vacuum calculations. For the β-anomer, vacuum and PCM calculations gave rise to the same global minimum, namely that with a counterclockwise arrangement of hydrogen bonds (**gGgg gG**). Other low energy conformers (Table 3) have a similar conformation, and were also privileged in vacuum calculations. On the other hand, these two stable conformations (**GTgg gG** for α-galactose, **gGgg gG** for β-galactose) are ranked second in free energy calculations with SMD (Table 3), but most of the remaining SMD stable conformers do not appear as stable vacuum conformers. These results indicate that even using a solvent model like PCM and optimizing the geometry, calculations lead to conformers with some degree of cooperative hydrogen bond arrangement. This makes sense, since a continuum method is not realistically modeling hydrogen bond interactions with the solvent, thus keeping the original, intramolecular hydrogen bonds. SMD shows a lower tendency for keeping these conformers. In any

Table 3
The three most stable conformers for the $^4C_1$ shape of solvated α- and β-D-galactopyranose, calculated using different methods.

Conformer	Relative energy (kcal/mol)[a]								
	B3LYP ΔG SMD	B3LYP ΔE SMD	M06-2X ΔG SMD	M06-2X ΔE SMD	B3LYP ΔG PCM	B3LYP ΔE PCM	M06-2X ΔG PCM	M06-2X ΔE PCM	MM3 ε = 80
α-D-Gal*p*									
GTGg gG	0.00 (1)		0.00 (1)						
GTgg gG	0.21 (2)	0.17 (3)	0.00 (2)		0.00 (1)	0.21 (2)	0.00 (1)	0.37 (3)	
GTGg gg	0.56 (3)								
GTgT gG			0.10 (3)						
GTTT gG		0.00 (1)		0.19 (3)					
GTTG Gg		0.10 (2)		0.00 (1)	0.68 (3)	0.25 (3)	0.41 (2)	0.25 (2)	
GTgg GG				0.18 (2)	0.35 (2)	0.00 (1)	0.41 (3)	0.00 (1)	
GGgg gT									0.00 (1)
GgGg gT									0.02 (2)
Gggg gT									0.10 (3)
β-D-Gal*p*									
TGgg gG	0.00 (1)				0.49 (3)		0.54 (3)		
gGgg gG	0.31 (2)		0.06 (2)		0.00 (1)	0.05 (2)	0.00 (1)	0.20 (3)	0.21 (2)
TGTG gG	0.51 (3)								
gGTT gG		0.00 (1)	0.39 (3)	0.00 (1)					
TGTT gG		0.18 (2)		0.24 (3)					
ggTT gG		0.25 (3)	0.00 (1)						
gGTG Gg				0.24 (2)		0.18 (3)		0.15 (2)	
gGgg GG					0.32 (2)	0.00 (1)	0.22 (2)	0.00 (1)	
gGgg gT									0.00 (1)
ggGg gT									0.22 (3)

[a] Rank number for each conformer is given in parenthesis.

case, many more conformers were found, because these interactions are weakened. On the other hand, MM3 calculations at ε = 80 do not reproduce at all the results obtained at ε = 1.5, especially for the α-anomer. The most stable conformers at high dielectric constant (Table 3) appear very low in the ranking of vacuum calculations. With the β-anomer, results are less straightforward: the two most stable structures correspond to those ranked fifth and first, respectively, in the vacuum calculations. Other stable conformers (Table 3) are much less important in those calculations. Comparison with the vacuum calculations of the mean absolute deviations (MAD) and the ranges of relative difference (RRD) between models (Table 2) also explain some of the observed trends. The MAD values for MM3 against the four DFT calculations for the α-anomer are 1.53–2.13 kcal/mol with PCM and 0.99–1.24 kcal/mol with SMD, whereas they are 0.94–1.32 kcal/mol (PCM) and 0.90–1.09 kcal/mol (SMD) for the β-anomer. The values are roughly similar to those observed in vacuum calculations for the β-anomer, whereas they show a decreasing trend vacuum > PCM > SMD for the α-anomer (Table 2). In all cases, lower MADs for the β-anomer are observed. The sign of the MDs indicate that MM3 tends to give lower energy values in all PCM calculations, vacuum calculations for α-galactose, and free energy SMD calculations, but higher values when comparing with electronic energy SMD calculations, and vacuum calculation with β-galactose. On the other hand, the comparisons between both DFT methods give much lower MADs (0.12–0.52 kcal/mol for both anomers) and RRDs (0.71–2.77 kcal/mol). The SMD calculations give particularly similar results for both functionals, at least using electronic energies (Table 2, MADs of 0.12–0.14 kcal/mol). As occurred with vacuum calculations, by the PCM model B3LYP tends to give a shorter span of energy values, as indicated by the negative sign of the MDs, suggesting a better stabilization of the global minimum. However, using SMD this trend is slightly reversed. The comparison of free and electronic energies gives rise usually to small differences, with a flattening of the free energy surfaces, as observed in vacuum calculations as well as in PCM water calculations (Table 2). However, the reverse trend is observed using SMD: free energy calculations give higher average energies and ranges, especially using B3LYP (Table 2).

3.4. Differences in exocyclic angles

The different models obviously led to different optimized geometries. Fine details of the precise geometry of the rings and puckering parameters are out of the scope of the current paper. However, as a full search of the different exocyclic angles was carried out, a comparative evaluation of their geometries may help to assess their variations. Table 4 shows the average differences for the six exocyclic angles between the B3LYP geometry and the other two geometries for all the conformers existing in both models. For both the vacuum and solvent calculations, no major differences between the results for α- and β-anomers are observed. As expected, the average difference between the DFT methods is lower, of only 2° in vacuum calculations, and slightly higher with the SMD and PCM models, whereas the difference with the classical method MM3 is larger, especially with the PCM solvent-modeled DFT conformers (ca. 6° for vacuum, ca. 7° for SMD, ca. 9° for PCM). However, not all angles contribute equally, especially in relation with MM3. Between the DFT methods in vacuum calculations, independent results for each angle indicate average differences of 1.4–2.7°, being χ_6 and ω those which vary more (2.4–2.7°) and χ_1 that with the lower variation (1.4–1.7°). For PCM calculations, these values rise to average differences of 1.3–4.0°, where ω shows the largest variation (4.0°) and χ_1 the lowest (1.3–1.8°). SMD gives rise to a more evenly distributed difference between angles (1.2–3.0°), but ω is still that showing the largest differences. On the other hand, when conferring MM3 and B3LYP vacuum geometries, χ_6 shows the largest variation (10.5–10.6°) followed by χ_4 (7.2–7.8°), whereas the remaining angles vary much less (3.5–3.7° for β-galactose, 3.1–5.7° for α-galactose). The main source of difference for the χ_6 angle occurs with some $\omega\chi_6$ = **GG** combinations, which either carry

Table 4
Average differences in exocyclic torsion angles[a] between different models and between each model and a perfectly staggered[a,b] conformation (in degrees).

	α-Gal, vacuum	β-Gal, vacuum	α-Gal, SMD	β-Gal, SMD	α-Gal, PCM	β-Gal, PCM
Between models						
B3LYP vs M06-2X	2.0 ± 1.7	2.0 ± 1.6	2.5 ± 1.7	2.1 ± 1.7	2.7 ± 2.8	2.4 ± 2.9
B3LYP vs MM3	5.9 ± 4.8	5.5 ± 5.0	6.8 ± 7.5	7.3 ± 7.4	9.4 ± 8.6	8.6 ± 8.6
With perfect staggering						
B3LYP	13.9 ± 7.2	11.7 ± 7.7	11.1 ± 6.4	10.3 ± 6.5	14.2 ± 8.4	11.2 ± 8.0
M06-2X	13.3 ± 6.9	11.6 ± 7.4	10.5 ± 6.9	9.6 ± 6.9	13.0 ± 7.6	10.5 ± 6.9
MM3	14.1 ± 10.3	12.6 ± 10.4	10.9 ± 9.1	9.8 ± 9.6		

[a] Average of the differences in angles χ_n with n = 1, 2, 3, 4 and 6, and ω ± the standard deviation.
[b] The lowest value of the difference of each dihedral angle with +60, −60 and 180° was considered for the calculation.

values of ca. −45° or values of −60°. MM3 optimize the first ones into a more eclipsed arrangement (χ_6 between 0 and −25°) and the second ones towards the other side (χ_6 around −80°). For the χ_4 angle the difference arises mainly from conformers with $\chi_4\omega\chi_6$ = **GGg**, where χ_4 has a value of ca. −90° with DFT, and of −60°–−70° with MM3, probably related with the DFT methods adopting the best angle for the H(O)-4 ⋯ O-6 hydrogen bond. With either solvent modeling, the differences increase considerably. Always χ_4 shows the largest variation (14.8–15.8°), mostly originated in the same conformers mentioned earlier ($\chi_4\omega\chi_6$ = **GGg**). The difference is larger in this case, because the DFT methods keep χ_4 with the −90° value, but MM3 shifts it to −40°. The angle showing the second largest variation is χ_3 in PCM calculations, and χ_6 in SMD calculations, for both anomers. The angle ω always shows little variation, of about 3° in average.

The other difference that has been investigated corresponds to that of the real angle values and those expected from a perfectly staggered conformation (±60°, 180°). The data are also shown on Table 4. Results indicate that with every model, the difference appears larger for α-Gal than for β-Gal, especially in vacuum and PCM calculations. However, a detailed analysis of the data (with the exception of MM3 at ε = 80) indicates that for these models, this is originated in a higher dispersion of the values for the χ_1 and χ_2 angles, closer to the anomeric center. The variations for χ_2 are just 6.1–7.4° for the β-anomer, whereas they rise to 15.4–18.7° for the α-anomer. Less pronounced are the variations for χ_1: 7.8–10.3° to 9.9–16.5°. Results are similar when comparing vacuum and PCM calculations. For the SMD calculations, χ_1 is the main source of distinction: the difference is 13.1–13.9° for the β-anomer, and 16.4–17.1° for the α-anomer. In all the methods, the largest variations with perfect staggering are observed for the χ_4 angle, which differs in 16.1–22.3°. The χ_3 angle shows a large variation from staggering in vacuum calculations (15.8–20.1°), but it decreases when water is modeled (8.8–16.5°). As explained earlier, the χ_1 and χ_2 angles show a large dispersion for the α-anomer, but not for the β-anomer. The lowest variation is usually observed for the ω angle, which as expected, is a "harder" dihedral angle, with heavier atoms across. The average variation is only 3.0–5.2° with MM3, 3.9–5.3° with the SMD model, and rises to 4.7–7.4° with the DFT vacuum or PCM models. It might have been expected that the variations should have been smaller for MM3, which has explicit sinusoidal functions to stabilize angles closer to the ideal value, than for DFT methods. However, a closer look at the actual torsional potential functions involved for the C–C–O–H and H–C–O–H angles determine that they have small effects: H–C–O–H has minima at ± 60 and 180°, but with an energy difference of only 0.2 kcal/mol with the maxima. The C–C–O–H dihedral angle has only a minimum at 180°, whereas at the *gauche* positions only a couple of shoulders are observed, with a total energy span of 0.5 kcal/mol. The effect might be more marked for the angle ω, as the function for the dihedral angle O–C–C–O has a total span of 3.7 kcal/mol. However, the global minima do not appear exactly at 60°, but at ± 70.5°. The function for C–C–C–O is softer (0.5 kcal/mol), but gives minima at ± 63.8 and 180°. Thus, for MM3 the trend to give angles closer to the ideally staggered is not strong enough.

3.5. Population analysis

The results of vacuum calculations can be compared to experimental data as the crystal structure or conformer population by a combination of resonant two-photon ionization and resonant ion-dip IR spectroscopy [26,27]. On the other hand, it is hard to know if the ensembles of conformers obtained with the solvent models represent the dynamic structure of the sugar in aqueous solution. In that sense, a hint can be obtained by comparing the experimentally retrieved data on anomeric equilibrium or hydroxymethyl rotameric ratio with that deduced from the Boltzmann-averaged data for the ensembles. We have used the free energies and the Boltzmann equation to determine the population of different conformers (or even anomers) in the equilibrium. Table 5 shows the results and comparisons with experimental data in solution. Regarding the difference between the anomers, as expected from the magnitude of the anomeric effect, DFT methods show that the most stable conformer of the α-anomer has less energy than that of the β-anomer. The difference in vacuum calculations is 2.21–3.33 kcal/mol (higher by M06-2X than by B3LYP), but it decreases by ca. 1 kcal/mol when free energies are considered. PCM solvent modeling decreases further the difference, in such a way that B3LYP gives a similar free energy for the most stable conformer of each anomer. SMD solvent modeling decreases the differences even further, thus making the β-anomer as the most stable (Table 5). The dampening of the anomeric effect in water is a known fact [46]. MM3 does not model so good the anomeric effect, and thus the β-anomer appears better stabilized. The experimental α/β ratio in aqueous solution is 34:66 [47,48]. The results with the different solvent models show an evident trend: PCM tends to underestimate the effect of the solvent. Thus, the increase in the population of the β-anomers is not enough to reach the experimental value. However, as B3LYP stabilizes better the β-anomers than M06-2X, a fair agreement with that ratio (43:57, Table 5) is observed with B3LYP. On the other hand, SMD tends to overestimate the solvation effect. In this case, M06-2X, which stabilizes better the α-anomers than B3LYP, gives a fair agreement with the experimental ratio (30:70, Table 5). Application of the COSMO solvent model to some rotamers (not the whole ensemble) was reported to give a better agreement [48]. Another important population ratio corresponds to the conformation of the exocyclic hydroxymethyl groups. There are several experimental determinations made for galactose and its glycosides [42–45,48,49], with different values. As an average, for both anomers, a *gg:gt:tg* ratio of about 15:64:21 was observed in water (Table 5). Most of the determinations were obtained using NMR three bond H–H coupling constants [42–44]. However, further determinations by the group of Serianni using a combination of different coupling

Table 5
Population of different rotamers and anomers, and energy difference between most stable rotamers for each anomer.

	α-Galp, vacuum	β-Galp, vacuum	α-Galp, water	β-Galp, water
Ratio gg:gt:tg[a]				
B3LYP	54:32:13	18:60:22	36:48:16 (PCM) 12:77:11 (SMD)	31:50:19 (PCM) 8:77:15 (SMD)
M06-2X	74:19:13	29:47:24	46:41:13 (PCM) 12:76:12 (SMD)	40:46:13 (PCM) 11:74:15 (SMD)
MM3	49:49:2	42:56:2	14:82:4	13:82:5
Experimental[b]				
Free sugar, ref. [42]			17:63:20	18:62:20
Free sugar, ref. [43]			18:38:44	24:66:10
Free sugar, ref. [44]				19:65:17
Me glycoside, ref. [42]			13:70:17	17:65:18
Me glycoside, ref. [43]			14:66:20	21:61:18
Me glycoside, ref. [44]			16:75:9	18:57:26
Me glycoside, ref. [45]			3:74:23	3:72:25
Population of rotamers favored by exo-anomeric effect[c] *(%)*				
B3LYP	51.8	60.2	85.8 (PCM) 92.9 (SMD)	69.3 (PCM) 51.6 (SMD)
M06-2X	30.6	51.8	83.0 (PCM) 93.5 (SMD)	68.4 (PCM) 58.4 (SMD)
MM3	96.9	84.7	97.6	81.4
Population of α-anomers (%)				
B3LYP	79.9		43.5 (PCM) 15.2 (SMD)	
M06-2X	95.2		73.2 (PCM) 29.6 (SMD)	
MM3	44.2		24.2	
Experimental			34	
$\Delta E_{\alpha-\beta}$ *(kcal/mol)*				
B3LYP	−2.21		−0.75 (PCM) +0.53 (SMD)	
M06-2X	−3.33		−1.32 (PCM) −0.31 (SMD)	
MM3	+0.13		+0.76	
$\Delta G_{\alpha-\beta}$ *(kcal/mol)*				
B3LYP	−0.97		−0.03 (PCM) +0.77 (SMD)	
M06-2X	−2.33		−0.72 (PCM) +0.39 (SMD)	

[a] It corresponds to the ratio of conformers with ω angles **G**:**g**:**T**.
[b] Determined by measurement of NMR coupling constants. Results from equation B were used when more than one was available.
[c] Only the rotamers with χ_1 = **G** for α-anomers, and **g** for β-anomers were considered.

constants on isotopically labeled compounds has disclosed the presence of only a few *gg* rotamers (Table 5) [45,50]. Vacuum calculations yield a ratio similar to that determined experimentally for the β-anomer, especially with B3LYP (Table 5). The *gg* proportion increases dramatically for the α-anomer (the most populated in vacuum, Table 5). This increase of gg rotamers in α-glycosides has already been noted [44,49], and explained in terms of an augmented *gauche*-effect [44,51]. Solvent modeling tends to equilibrate the ratios for both anomers (in part due to a decreased *gauche*-effect in solution [50]), showing a net increase of the *gt* conformers over the remaining ones. However, as observed for the anomeric population the PCM solvent model is insufficient to provide enough *gt* conformers to cope with the experimental results (Table 5), whereas the SMD solvent model matches quite well the results obtained experimentally by some of the different papers (Table 5). Only a slight overestimation of the *gt* rotamers is observed in some cases. There are no major differences between the functionals, although for PCM, B3LYP gives results slightly closer to the experimental values than M06-2X. Tvaroška et al. [49] have found a similar coincidence between calculated (*gg:gt:tg* ratios of 14:72:14 and 12:76:12 for the α- and β-methyl galactopyranosides, respectively) and experimental values using the solvent model implemented in Jaguar over a B3LYP/6-31G** calculation. However, the authors pointed out that they analyzed only a small slice of the potential energy surface and that thus, that the agreement may be fortuitous [49]. The major effects that determine the rotamer population of the hydroxymethyl groups are solvation effects, 1,3-diaxial interactions, the *gauche*-effect and hydrogen bonding [44]. The high proportion of *gg* rotamers in vacuum calculations is probably related to their high O-4···H···O-6 capabilities and to the *gauche*-effect, in spite of the unfavorable *syn*-diaxial arrangement [49]. In water, where the hydrogen bonds are dampened and the *gauche*-effect loses weight [49], the *gt* rotamers, with no O-4/O-6 hydrogen bonding capabilities become the most populated. As mentioned earlier, the SMD model is capable of reproducing these preferences, but PCM maintains the importance of hydrogen bonding and thus keeps a high population of *gg* rotamers.

The exo-anomeric effect stabilizes conformations where χ_1 is **G** for α-anomers, and **g** for β-anomers, for the same stereoelectronic grounds that stabilize axial polar groups in the anomeric carbon. Although this effect also acts on χ_1 = **T** rotamers, these are less important for sterical reasons. This effect is usually observed in the conformational maps of di- and oligosaccharides [52]. MM3 shows a large predominance of these rotamers (Table 5), at either dielectric constant, especially for the α-anomer. The DFT methods also show large populations of these rotamers, but mostly with the solvent models. It has already been stated [20] that the exo-anomeric effect is turned over by strong hydrogen bonds. This can explain why the population increases with solvent models: as

the hydrogen bond strength diminishes, the exo-anomeric effect acquires importance.

4. Conclusions

The aim of this paper is to establish a simple mechanism for the exhaustive search of the rotamers of molecules containing many exocyclic groups, like monosaccharides, and to compare the results produced by different calculation models. Herein, we have made full searches for the most stable chair conformations of α- and β-D-galactopyranose in gas phase and using solvent continuum models. The geometry optimizations and energy determinations have been carried out with the B3LYP and M06-2X functionals and the 6-311+G** basis set, using MM3 as the starting point. Free energies were also calculated. We expect that the current paper will not be limited to help researchers to determine starting points for their modeling work; other goals may come, for example, from unraveling how the presence of different rotamers may affect the polar and non-polar regions for molecular recognition events. Some interesting conclusions can be drawn from our results. The first ones arise from our vacuum calculations.

There are about one hundred stable rotamers for each compound within each model. They occupy ca. 14 kcal/mol of conformational space. Most of these conformers match their exocyclic angle orientations between models, but there are some, usually high-energy rotamers, which appear in some models and not in others.

For α-Gal*p*, the rotamer with a clockwise arrangement of hydrogen bonds, which extend to O-6 *via* a *gg* arrangement of the hydroxymethyl group (**ggTG Gg**) is the most stable by DFT calculations (Fig. 2a). Following this rotamer, others with a counterclockwise arrangement of hydrogen bonds appear second in importance, with a significant energy difference with the global minimum.

On the contrary, for β-Gal*p*, the most stable structure corresponds to that with a counterclockwise arrangement of hydrogen bonds (**gGgg gG**), with a *gt* arrangement of the hydroxymethyl group (Fig. 2b). There are many structures with low energy, most of them with small variants of the same arrangement. The conformer with a clockwise arrangement of H-bonds appears to be less important: although stabilized in electronic energy calculations by M06-2X, free energy calculations tend to disfavor it, as any B3LYP calculation does.

There are several numerical differences between the calculations for each anomer. Average electronic energies of the conformers are 6.6–7.4 kcal/mol for the α-anomer, and 5.0–5.3 kcal/mol the β-anomer. These figures decrease for both when free energies are calculated: 5.4–6.5 kcal/mol for the α-anomer, and 4.6–4.9 kcal/mol the β-anomer. The higher number of each range always corresponds to the M06-2X calculation. In any case the dissimilarities appear to be significantly higher for the calculations for α-Gal*p*: the mean absolute deviations between both DFT models fall from 0.65 to 0.91 kcal/mol for the α-anomer to 0.31–0.33 kcal/mol for the β-anomer. Comparison of free energies with electronic energies, it also decreases from α- to β-anomer from 0.90 to 1.16 kcal/mol to 0.52–0.55 kcal/mol. In all cases M06-2X calculations and electronic energy determinations tend to give higher energy ranges when compared to the reference conformer (the global minimum). In other words, the β-anomer appears to be modeled more evenly with both DFT models. Maybe, a different treatment of the anomeric effect is complicating the calculations of the α-anomer.

Solvation clearly introduces a flattening of the surfaces, but in different extents for each model. The average energies are reduced by about 2 kcal/mol with respect to the vacuum ensembles with PCM and by about 3–4 kcal/mol with SMD. The average electronic energies for the α-anomer are 4.2–4.6 kcal/mol with PCM, and 2.4–2.5 kcal/mol with SMD. For the β-anomer, they are 3.3–3.7 kcal/mol with PCM, and 1.9–2.0 kcal/mol with SMD. The calculation of free energies also generates a differential behavior with the solvent models: it produces an additional flattening of 0.2–0.5 kcal/mol with PCM, but they increase by 0.3–0.6 kcal/mol with SMD. The number of available rotamers for the solvated ensembles is considerably larger than that of the vacuum calculations. Almost 300 different rotamers have been identified by DFT methods for each anomer using PCM, and more than 400 using SMD.

DFT calculations with inclusion of solvent lead to some global minima which also appeared highly stabilized in vacuum calculations. The intramolecular hydrogen bond is still a stabilizing factor of the geometry optimization process even when the presence of water is modeled by the continuum method PCM. The SMD model gives rise instead to many new conformers, indicating a larger solvating effect. MM3 gives mostly different stable conformers at distinct dielectric constants.

Using PCM, the MAD values for MM3 against the four DFT calculations are 1.53–2.13 kcal/mol for the α-anomer, and 0.94–1.32 for the β-anomer, roughly similar to those observed in vacuum calculations for each anomer. Using SMD, the β-anomer showed the same trend, but for the α-anomer, a marked decrease in MAD values is observed (0.99–1.24 kcal/mol). Comparison between both DFT functionals give much lower MADs (0.12–0.52 kcal/mol for both anomers and methods) and RRDs (0.71–2.77 kcal/mol). These values are similar to those for vacuum calculations of β-galactose, but largely lower than those for the α-anomer. The MD values for the comparisons of electronic and free energies show that vacuum and PCM calculations show a flattened free energy surface (positive MDs), whereas SMD calculations give flattened electronic energy surfaces (negative MDs).

Only small differences in geometry were determined between the conformers found with each DFT model: about 2-3° in average for the exocyclic dihedral angles. As expected, this difference is multiplied by 3 or 4 when comparing to the MM3 geometries. The angle χ_4 is the main source of difference, especially with the solvent models.

The calculated rotamer populations in solution put in evidence the behavior of the different solvent models: PCM still keeps many of the stabilizing factors observed in vacuum calculations, thus underestimating the solvent effect. On the other hand, the SMD model gives a better picture of the solvation effects. The α/β anomeric ratio is underestimated by SMD and overestimated by PCM. As B3LYP stabilize differentially better the β-anomers, fair agreements with experimental anomeric ratio upon mutarotation are observed with B3LYP+PCM, or with M06-2X+SMD. In terms of hydroxymethyl group rotamers, a similar trend is observed: PCM underestimates the proportion of *gt* rotamers (more stable in solution), whereas SMD states correctly this proportion.

Acknowledgments

The authors thank the Consejo Nacional de Investigaciones Científicas y Técnicas (PIP 699/11 and 298/14), the Agencia Nacional de Promoción Científica y Tecnológica (PICT 2013/2088 and 2014/0471) and the Universidad de Buenos Aires (Q004 and Q203) for financial support. E.A.D.V. is a Fellow from the Consejo Nacional de Investigaciones Científicas y Técnicas (CONICET), Argentina. C.M. and C.A.S. are Research Members of the same Institution.

Appendix A. Supplementary data

Supplementary data related to this article can be found at http://dx.doi.org/10.1016/j.carres.2017.05.003.

References

[1] S. Pérez, Theoretical aspects of oligosaccharide conformation, Curr. Opin. Struct. Biol. 3 (5) (1993) 675–680.
[2] A.D. French, J.W. Brady, ACS Symp. Ser. 430 (1989) 1–19.
[3] H.B. Mayes, L.J. Broadbelt, G.T. Beckham, How sugars pucker: electronic structure calculations map the kinetic landscape of five biologically paramount monosaccharides and their implications for enzymatic catalysis, J. Am. Chem. Soc. 136 (3) (2014) 1008–1022.
[4] V.A. Cosenza, D.A. Navarro, C.A. Stortz, DFT/PCM theoretical study of the conversion of methyl 4-O-methyl-α-d-galactopyranoside 6-sulfate and its 2-sulfated derivative into their 3,6-anhydro counterparts, Carbohydr. Res. 426 (2016) 15–25.
[5] S. Melberg, K. Rasmussen, Conformations of disaccharides by empirical force-field calculations: Part I, β-maltose, Carbohydr. Res. 69 (1) (1979) 27–38.
[6] A.D. French, Comparisons of rigid and relaxed conformational maps for cellobiose and maltose, Carbohydr. Res. 188 (1989) 206–211.
[7] A. Imberty, V. Tran, S. Pérez, Relaxed potential energy surfaces ofN-linked oligosaccharides: the mannose-α(1 → 3)-mannose case, J. Comput. Chem. 11 (2) (1990) 205–216.
[8] I. Tvaroška, T. Kožar, M. Hricovíni, ACS Symp. Ser. 430 (1989) 162–176.
[9] S.N. Ha, L.J. Madsen, J.W. Brady, Conformational analysis and molecular dynamics simulations of maltose, Biopolymers 27 (12) (1988) 1927–1952.
[10] M. Martín-Pastor, J.F. Espinosa, J.L. Asensio, J. Jiménez-Barbero, A comparison of the geometry and of the energy results obtained by application of different molecular mechanics force fields to methyl α-lactoside and the C-analogue of lactose, Carbohydr. Res. 298 (1–2) (1997) 15–49.
[11] J. Koča, S. Pérez, A. Imberty, J. Comput. Chem. 16 (1995) 296–310.
[12] S.B. Engelsen, J. Koca, I. Braccini, C. Hervé du Penhoat, S. Pérez, Travelling on the potential energy surfaces of carbohydrates: comparative application of an exhaustive systematic conformational search with an heuristic search, Carbohydr. Res. 276 (1) (1995) 1–29.
[13] S.W. Homans, M. Forster, Application of restrained minimization, simulated annealing and molecular dynamics simulations for the conformational analysis of oligosaccharides, Glycobiology 2 (2) (1992) 143–151.
[14] K.-H. Ott, B. Meyer, Carbohydr. Res. 281 (1996) 11–34.
[15] R.K. Schmidt, M. Karplus, J.W. Brady, The anomeric equilibrium ind-xylose: free energy and the role of solvent structuring, J. Am. Chem. Soc. 118 (3) (1996) 541–546.
[16] W. Plazinski, M. Drach, A. Plazinska, Ring inversion properties of 1→2, 1→3 and 1→6-linked hexopyranoses and their correlation with the conformation of glycosidic linkages, Carbohydr. Res. 423 (2016) 43–48.
[17] W. Plazinski, A. Plazinska, M. Drach, Acyclic forms of aldohexoses and ketohexoses in aqueous and DMSO solutions: conformational features studied using molecular dynamics simulations, Phys. Chem. Chem. Phys. PCCP 18 (14) (2016) 9626–9635.
[18] A. Ardèvol, X. Biarnés, A. Planas, C. Rovira, The conformational free-energy landscape of β-D-mannopyranose: evidence for a (1)S(5) → B(2,5) → (O)S(2) catalytic itinerary in β-mannosidases, J. Am. Chem. Soc. 132 (45) (2010) 16058–16065.
[19] P.L. Polavarapu, C.S. Ewig, Ab Initio computed molecular structures and energies of the conformers of glucose, J. Comput. Chem. 13 (10) (1992) 1255–1261.
[20] C.J. Cramer, D.G. Truhlar, Quantum chemical conformational analysis of glucose in aqueous solution, J. Am. Chem. Soc. 115 (13) (1993) 5745–5753.
[21] F. Zuccarello, G. Buemi, A theoretical study of d-glucose, d-galactose, and parent molecules: solvent effect on conformational stabilities and rotational motions of exocyclic groups, Carbohydr. Res. 273 (2) (1995) 129–145.
[22] C.A. Stortz, An. Asoc. Quim. Argent. 86 (1998) 94–103.
[23] M. Rahal-Sekkal, N. Sekkal, D.C. Kleb, P. Bleckmann, J. Comput. Chem. 24 (2002) 806–818.
[24] F.A. Momany, M. Appell, J.L. Willett, U. Schnupf, W.B. Bosma, DFT study of alpha- and beta-D-galactopyranose at the B3LYP/6-311++G** level of theory, Carbohydr. Res. 341 (4) (2006) 525–537.
[25] Y.K. Sturdy, C.K. Skylaris, D.C. Clary, Torsional anharmonicity in the conformational analysis of beta-D-galactose, J. Phys. Chem. B 110 (8) (2006) 3485–3492.
[26] R.A. Jockusch, F.O. Talbot, J.P. Simons, Sugars in the gas phase, Phys. Chem. Chem. Phys. 5 (8) (2003) 1502–1507.
[27] P. Çarçabal, R.A. Jockusch, I. Hünig, L.C. Snoek, R.T. Kroemer, B.G. Davis, D.P. Gamblin, I. Compagnon, J. Oomens, J.P. Simons, J. Am. Chem. Soc. 127 (2005) 11414–11425.
[28] N.L. Allinger, Y.H. Yuh, J.H. Lii, Molecular mechanics. The MM3 force field for hydrocarbons. 1, J. Am. Chem. Soc. 111 (23) (1989) 8551–8566.
[29] N.L. Allinger, M. Rahman, J.H. Lii, J. Am. Chem. Soc. 112 (1990) 8293–8307.
[30] A.D. Becke, Density-functional thermochemistry. III. The role of exact exchange, J. Chem. Phys. 98 (7) (1993) 5648–5652.
[31] Y. Zhao, D.G. Truhlar, The M06 suite of density functionals for main group thermochemistry, thermochemical kinetics, noncovalent interactions, excited states, and transition elements: two new functionals and systematic testing of four M06-class functionals and 12 other functionals, Theor. Chem. Acc. 120 (1–3) (2008) 215–241.
[32] J. Tomasi, B. Mennucci, R. Cammi, Quantum mechanical continuum solvation models, Chem. Rev. 105 (8) (2005) 2999–3093.
[33] A.V. Marenich, C.J. Cramer, D.G. Truhlar, Universal solvation model based on solute electron density and on a continuum model of the solvent defined by the bulk dielectric constant and atomic surface tensions, J. Phys. Chem. B 113 (18) (2009) 6378–6396.
[34] C.A. Stortz, Comparative performance of MM3(92) and two TINKER MM3 versions for the modeling of carbohydrates, J. Comput. Chem. 26 (5) (2005) 471–483.
[35] M.J. Frisch, G.W. Trucks, H.B. Schlegel, G.E. Scuseria, M.A. Robb, J.R. Cheeseman, G. Scalmani, V. Barone, B. Mennucci, G.A. Petersson, H. Nakatsuji, M. Caricato, X. Li, H.P. Hratchian, A.F. Izmaylov, J. Bloino, G. Zheng, J.L. Sonnenberg, M. Hada, M. Ehara, K. Toyota, R. Fukuda, J. Hasegawa, M. Ishida, T. Nakajima, Y. Honda, O. Kitao, H. Nakai, T. Vreven, J.A. Montgomery, J.E. Peralta, F. Ogliaro, M. Bearpark, J.J. Heyd, E. Brothers, K.N. Kudin, V.N. Staroverov, R. Kobayashi, J. Normand, K. Raghavachari, A. Rendell, J.C. Burant, S.S. Iyengar, J. Tomasi, M. Cossi, N. Rega, J.M. Millam, M. Klene, J.E. Knox, J.B. Cross, V. Bakken, C. Adamo, J. Jaramillo, R. Gomperts, R.E. Stratmann, O. Yazyev, A.J. Austin, R. Cammi, C. Pomelli, J.W. Ochterski, R.L. Martin, K. Morokuma, V.G. Zakrzewski, G.A. Voth, P. Salvador, J.J. Dannenberg, S. Dapprich, A.D. Daniels, Ö. Farkas, J.B. Foresman, J.V. Ortiz, J. Cioslowski, D.J. Fox, Gaussian 09, Revision C.01, Gaussian, Inc., Wallingford CT, 2009.
[36] G.I. Csonka, A.D. French, G.P. Johnson, C.A. Stortz, Evaluation of density functionals and basis sets for carbohydrates, J. Chem. Theory Comput. 5 (4) (2009) 679–692.
[37] J. Ohanessian, H. Gillier-Pandraud, Acta Cryst. B 32 (1976) 2810–2813.
[38] L.C.E. Kouwijzer, V.P. van Eijck, H. Kooijman, J. Kroon, Acta Cryst. B 51 (1995) 209–220.
[39] G.I. Csonka, J.G. Ángyán, The origin of the problems with the PM3 core repulsion function, J. Mol. Struct. Theochem. 393 (1–3) (1997) 31–38.
[40] F. Longchambon, J. Ohanessian, D. Avenel, A. Neuman, Acta Cryst. B 31 (1975) 2623–2627.
[41] M. Kinoshita, in: F. Hirata (Ed.), Molecular Theory of Solvation, Kluwer, Dordrecht, 2003, pp. 101–168.
[42] H. Ohrui, Y. Nishida, H. Higuchi, H. Hori, H. Meguro, The preferred rotamer about the C5—C6bond ofD-galactopyranoses and the stereochemistry of dehydrogenation byD-galactose oxidase, Can. J. Chem. 65 (6) (1987) 1145–1153.
[43] K. Bock, H. Thøgersen, Annu. Rep. NMR Spectrosc. 13 (1983) 1–57.
[44] K. Bock, J.Ø. Duus, J. Carbohydr. Chem. 13 (1994) 513–543.
[45] C. Thibadeau, R. Stenutz, B. Hertz, T. Klepach, S. Zhao, Q. Wu, I. Carmichael, A.S. Serianni, J. Am. Chem. Soc. 126 (2004) 15668–15685.
[46] C. Wang, F. Ying, W. Wu, Y. Mo, How solvent influences the anomeric effect: roles of hyperconjugative versus steric interactions on the conformational preference, J. Org. Chem. 79 (4) (2014) 1571–1581.
[47] Y. Zhu, J. Zajicek, A.S. Serianni, Acyclic forms of [1-(13)C]aldohexoses in aqueous solution: quantitation by (13)C NMR and deuterium isotope effects on tautomeric equilibria, J. Org. Chem. 66 (19) (2001) 6244–6251.
[48] U. Schnupf, J.L. Willett, F. Momany, DFTMD studies of glucose and epimers: anomeric ratios, rotamer populations, and hydration energies, Carbohydr. Res. 345 (4) (2010) 503–511.
[49] I. Tvaroska, F.R. Taravel, J.P. Utille, J.P. Carver, Quantum mechanical and NMR spectroscopy studies on the conformations of the hydroxymethyl and methoxymethyl groups in aldohexosides, Carbohydr. Res. 337 (4) (2002) 353–367.
[50] R. Stenutz, I. Carmichael, G. Widmalm, A.S. Serianni, Hydroxymethyl group conformation in saccharides: structural dependencies of (2)J(HH), (3)J(HH), and (1)J(CH) spin-spin coupling constants, J. Org. Chem. 67 (3) (2002) 949–958.
[51] E. Juaristi, S. Antúnez, Conformational analysis of 5-substituted 1,3-dioxanes. 6. Study of the attractive gauche effect in O-C-C-O segments, Tetrahedron 48 (29) (1992) 5941–5950.
[52] V.S.R. Rao, P.K. Qasba, P.V. Balaji, R. Chandrasekaran, Conformation of Carbohydrates, Hardwood Academic Publishers, Amsterdam, 1998, 359 pp.